Chromatographia
DOI 10.1007/s10337-017-3253-y

ORIGINAL

Synthesis of Fe_3O_4@m-SiO_2/PSA@Zr-MOF Nanocomposites for Bifenthrin Determination in Water Samples

Mei Xu[1] · Kun Chen[1] · Chen Luo[2] · Guoxin Song[1] · Yaoming Hu[1] · Hefa Cheng[3]

Received: 4 August 2016 / Revised: 10 January 2017 / Accepted: 12 January 2017

Abstract In this paper, a simple but efficient method for the extraction and analysis of bifenthrin in water samples was proposed. The Fe_3O_4-based nanocomposites (Fe_3O_4@m-SiO_2/PSA@Zr-MOF) were successfully synthesized and developed as adsorbents for magnetic solid-phase extraction. With the solvothermal reaction and sol–gel method, the resultant adsorbents exhibited excellent characteristics of large surface areas, homogeneous pore size, strong magnetic responsivity and high hydrophilicity. The parameters affecting the extraction performance including adsorbent amounts, adsorption time, species of eluents and desorption time were investigated. Under the optimal conditions, validation experiments such as recovery, reproducibility and limits of detection (LOD) were carried out and showed satisfactory results. The LOD of the targeted analytes was found to be 0.5 μg L^{-1}. The average recovery was 103.2% with the intra-day and inter-day relative standard deviations of 2.0 and 3.5%, respectively. Ultimately, the novel magnetic adsorbents were successfully applied to detect the bifenthrin compound in real water samples.

✉ Guoxin Song
gxsong@fudan.edu.cn

✉ Yaoming Hu
ymhu@fudan.edu.cn

[1] Research Center of Analysis and Measurement, Fudan University, Shanghai 200433, China

[2] Shanghai Tobacco Group CO., LTD, 717 Changyang Road, Shanghai 200082, China

[3] College of Urban and Environmental Sciences, Peking University, Beijing 100871, China

Keywords GC–MS · Bifenthrin · Nanocomposites · Magnetic solid-phase extraction · Water samples

Introduction

Pesticides are widely used for the suppression of unwanted weeds and removal of nuisance insects/fungi in agricultural production systems [1, 2]. Currently, most pesticides used are biodegradable, and the extent of biodegradation depends mainly on their composition and chemical structures. Bifenthrin which belongs to pyrethroid chemical class can be persistent in the environment for a long time [3, 4]. In the growing season, bifenthrin is easily mobilized with loose soil particles into runoff and then enter downstream surface aquatic ecosystems. The presence of detectable concentrations of pesticides in surface water has caused some concerns about possible negative effects on human as well as aquatic biology [5, 6]. For bifenthrin, the acceptable daily intake is established at the level of 0.015 mg kg^{-1} of body weight [7]. Therefore, the determination for the contents of bifenthrin in water environments is greatly desirable. Gas chromatography (GC) and liquid chromatography (LC) coupled with mass spectrometry (MS) are the two frequently used techniques for the analysis. Due to the complicated environment matrix and the low content of targeted analytes, it is difficult to obtain good sensitivity while analyzing the compounds directly. As a consequence, sample pretreatment procedures are required. The commonly used pretreatment procedures are liquid–liquid extraction (LLE) and solid-phase extraction (SPE). However, these procedures are always laborious, time-consuming and sometimes requiring large dosages of toxic organic solvents [8–10]. The development of magnetic materials has generated a new mode of SPE called

Published online: 20 January 2017

magnetic solid-phase extraction (MSPE), which possesses an array of advantages such as high speed, compatibility and outstanding selectivity [11, 12].

With regard to the MSPE procedure, the first issue to be resolved is the choice of magnetic adsorbents. Normally, magnetic adsorbents are synthesized by modifying magnetic nanoparticles (MNPs) with special functional ligands through silylation, esterification, Lewis acid/base interaction, coordination, etc. [13, 14]. Mixed functional ligands on MNPs surface can endow them high adsorption ability toward the targeted analytes in the aqueous matrix. Among the various MNPs (i.e., iron, nickel, cobalt and their oxides) offered, iron oxides such as magnetite (Fe_3O_4) and maghemite (γ-Fe_2O_3) are widely used due to their super magnetic responsiveness [15, 16]. However, these iron oxides always easily aggregate and hardly suspend in aqueous phase due to their hydrophobicity and electron-rich features. To improve their dispersibility in the aqueous matrix, hydrophilic ligands are imported such as dopamine [17] and *N*-vinyl-2-pyrrolidone (NVP) [18]. In addition, the iron oxides are not fully selective when analyzing the targeted compounds directly. To overcome this drawback, the surfaces of iron oxides are usually modified with other functional ligands, such as C18 groups [19], graphene [20], carbon nanotubes [21] and metal–organic frameworks (MOFs) [22]. Here, MOFs are an interesting class of hybrid materials which exist as infinite crystalline lattices with metal clusters and organic linkers, and possess accessible cages, tunnels and modifiable pores. Owing to their flexible designs of pore sizes, they have showed great potential as absorbents for the extraction of targeted compounds in the complicated matrix [23, 24].

Inspired by the above-mentioned information, iron oxides modified with mixed functional ligands may have an enhanced adsorption ability toward bifenthrin in the water matrix. Herein, we selected Fe_3O_4 MNPs as the magnetic cores and then combined with amorphous silica (m-SiO_2), *N*-(*n*-propyl)ethylenediamine (PSA) and Zr-MOFs. The novel Fe_3O_4-based nanocomposites (Fe_3O_4@m-SiO_2/PSA@Zr-MOF) were developed as the MSPE absorbents for the extraction and analysis of bifenthrin in water samples. Additionally, the extraction parameters and the method validation were also investigated in this work.

Experimental

Reagents and Materials

Iron chloride hexahydrate ($FeCl_3{\cdot}6\ H_2O$) and zirconium (IV) chloride ($ZrCl_4$) were purchased from Sinapharm Chemical Reagent Co. Ltd. Tetraethoxysilane (TEOS), cetyltrimethylammonium bromide (CTAB), *N*-(*n*-propyl) ethylenediamine (PSA) and *N*,*N*-dimethylformamide (DMF) were obtained from Aladdin Industrial Co., Ltd. All the other reagents were of analytical grade and used without further purification unless otherwise mentioned. In addition, the deionized water was purified with a Milli-Q system (Milford, MA, USA).

Bifenthrin standard (1000 μg mL^{-1}) was purchased from the Shanghai Pesticide Research Institute. The standard stock solution of bifenthrin was prepared by dissolving bifenthrin into *n*-hexane with the concentration of 10 μg mL^{-1}. An internal standard of 10 μg mL^{-1} was obtained by dissolving a certain amount of tribromobiphenyl (TriBB) into *n*-hexane. Pond water samples were collected from the Handan campus of Fudan University (Shanghai, China); river water samples were collected from Jiading District (Shanghai, China). After filtering through a 0.45-μm membrane, they were stored at 4 °C before analysis.

Synthesis of Fe_3O_4@m-SiO_2/PSA@Zr-MOF

The Fe_3O_4@m-SiO_2/PSA@Zr-MOF nanocomposites were prepared following the diagrammatic approach shown in Fig. 1. It could be found that the nanocomposites were synthesized in three successive steps. Firstly, the magnetic Fe_3O_4 cores were obtained through a solvothermal reaction according to our previous work [18]. Briefly, $FeCl_3{\cdot}6H_2O$ (1.35 g) was dispersed into 75 mL ethylene glycol solution under magnetic stirring for 0.5 h. Then 3.6 g sodium acetate (NaAc) was added and stirred for 1 h. The mixture was transferred into a Teflon-lined stainless steel autoclave. The autoclave was carefully sealed and heated in a vacuum oven at 200 °C for 12 h. The black Fe_3O_4 cores were collected by magnetic separation, then washed with ethanol and dried in a vacuum at 50 °C.

Secondly, 50 mg Fe_3O_4 MNPs were mingled together with 500 mg CTAB into 50 mL deionized water, and the mixture was ultrasonically treated to form a homogeneous dispersion. The dispersive solution was mixed with 450 mL diluted NaOH solution, further ultrasonicated for 5 min, and heated at a preheated water bath (60 °C) for 30 min under mechanical stirring. Afterward, 2.5 mL TEOS/ethanol (v/v: 1/4) solution was introduced drop by drop, followed by heating at 60 °C for another 30 min. Subsequently, 200 μL TEOS/PSA (v/v: 1/1) mixture was injected into the dispersion and the reaction was allowed to continue at 60 °C for 12 h. The resultant products (labeled as Fe_3O_4@m-SiO_2/PSA) were collected, rinsed with deionized water, and refluxed in acetone to remove the CTAB templates thoroughly. The Fe_3O_4@m-SiO_2/PSA nanocomposites were vacuum dried at 50 °C overnight for further usage. Notably, the m-SiO_2 layer on the magnetic Fe_3O_4 cores had two functions: (I) providing a silica-like surface for Fe_3O_4 cores, which made the surface modification with

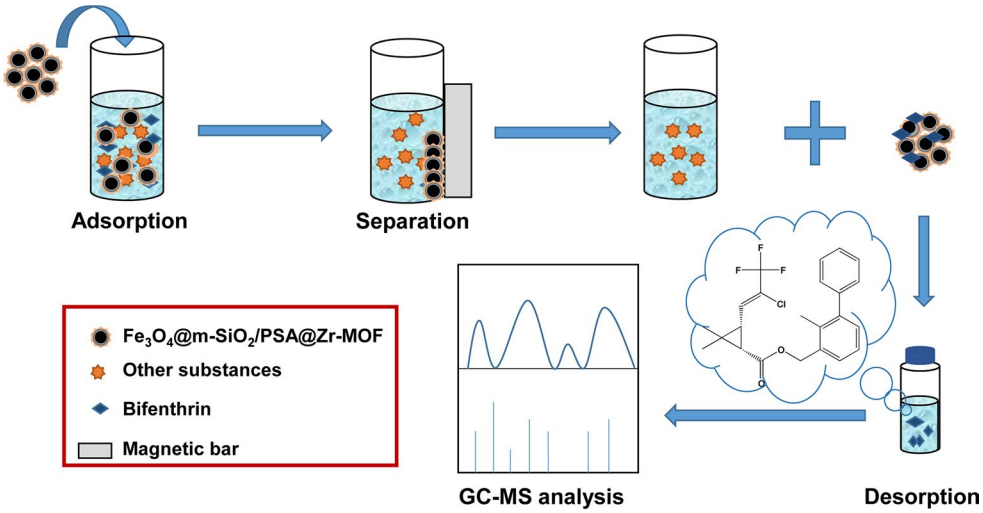

Fig. 1 Schematic illustration of the fabrication of Fe_3O_4@m-SiO_2/PSA@Zr-MOF nanocomposites (the dimension is not drawn to scale)

the following organic molecules easier; and (II) protecting the interior magnetic cores from being etched in practical applications.

Ultimately, 100 mg Fe_3O_4@m-SiO_2/PSA nanocomposites were redispersed in 40 mL DMF solution, and then 78 mg $ZrCl_4$ and 10 mg terephthalic acid were added. The prepared mixture was heated at 140 °C for 20 min. The resultant products (labeled as Fe_3O_4@m-SiO_2/PSA@Zr-MOF) were collected by magnetic separation, followed by rinsing with deionized water and methanol, and dried in a vacuum oven at 50 °C.

Instruments and Chromatographic Analytical Conditions

Scanning electron micrographs (SEM) were obtained by using Philips XL 30 electron microscope. Herein, the sizes of the resultant nanocomposites were measured in the "Nano Measurer" program using the corresponding SEM image. Sizes from 50 different nanocomposites were measured, and then average value and standard deviation were calculated [25]. Transmission electron microscopy (TEM) images and energy-dispersive X-ray (EDX) spectra were taken on a JEOL 2011 microscope (Japan) performed at 200 kV. Fourier transform infrared spectra (FT-IR) were collected on Nicolet Nexus 470 spectrophotometer using KBr pellets. X-ray photoelectron spectroscopy (XPS) was carried out on an RBD-upgraded PHI-5000C ESCA system (Perkin Elmer) with a Mg Kα source at 14.0 kV and 25 mA. The binding energies were calibrated using the containment carbon (C1s = 284.60 eV). Peak fitting was carried out for high-resolution N signals according to Shirley-type background subtraction (Shirley, 1972) using curve fitting XPSPEAK 4.1 program with Gaussian–Lorentzien 40%. X-ray diffraction (XRD) patterns (2θ ranges from 20° to 80°) were recorded at room temperature with scanning speed of 4°/min using Cu Kα radiation (λ = 1.540 Å) from a 40 kV X-ray source.

A Focus GC system, combined with a Thermo DSQ quadrupole mass spectrometer (Thermo Fisher Scientific, TX, USA) was used. The extracted compounds were separated by using HP-5MS (Agilent Technology, CA, USA) capillary column (30 m × 0.25 mm, 0.25 μm film). The extraction solvent after MSPE was injected directly in the splitless mode. The column oven temperature was programmed as follows: the initial temperature was 60 °C and lasted for 2 min; then it increased to 300 °C at a rate of 30 °C min^{-1} and was maintained at 300 °C for 5 min. Helium (99.999%) was utilized as the carrier gas with a flow rate of 1.0 mL min^{-1}. Electron impact ionization (EI) with nominal electron energy of 70 eV was used and the injection temperature was set at 250 °C. All samples were analyzed in the selected ion monitoring (SIM) mode. The retention time and mass to charge (m/z) of the characteristic ions for bifenthrin compound were as follows: time = 11.02 min; m/z = 165, 181, 422.

Optimization of MSPE Parameters

15 mL deionized water containing 10 μg mL^{-1} bifenthrin standard solution was added in a vial with PTFE–silicone septum. Then Fe_3O_4@m-SiO_2/PSA@Zr-MOF nanocomposites (15, 30 and 50 mg) were added into the vial to extract the targeted analytes by vortex for several adsorption times (3, 5, 10 and 15 min). A magnetic bar was attached to the outside sidewall of the vial to gather the adsorbents, and the supernatant was discarded. Subsequently, 1 mL desorption solution (acetone, acetonitrile and dichloromethane) and 0.5 g anhydrous $MgSO_4$ were introduced to the vial to elute the targeted analytes from the adsorbents under ultrasonic vibration for a certain time (3, 5 and 10 min). Here, anhydrous $MgSO_4$ acted as

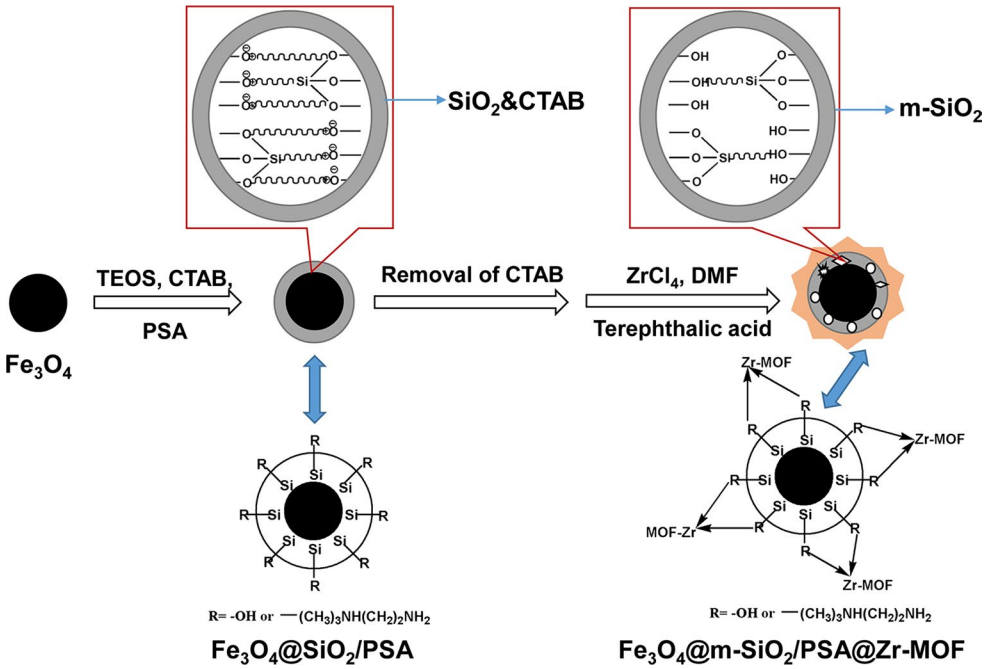

Fig. 2 Experimental MSPE procedure using the Fe_3O_4@m-SiO_2/PSA@Zr-MOF nanocomposites

drying agent to remove the residual water. Finally, 0.4 mL the supernatant was transferred into a 1.5-mL vial followed by the addition of 20.0 μL internal standard (TriBB, 10 μg mL^{-1}). After a fully mixing, 1.0 μL of the solution was injected into the GC–MS for analysis. The workflow for bifenthrin enrichment is illustrated in Fig. 2.

Analytical Validations

A set of experiments in relation to the linearity, limit of detection (LOD), limit of quantification (LOQ), and reproducibility were performed to validate the proposed signal-to-noise (*S*/*N*) method. The linear regression analysis was performed from the standard calibration solutions by plotting the mean peak area ratios (*y*, targeted analytes/TriBB) versus concentrations (3.3–200 μg L^{-1}) of corresponding analytes (*x*). The LOD and LOQ were calculated as the concentrations corresponding to $S/N = 3$ and 10, respectively. The reproducibility of the method was determined by precision. Herein, the method precision was obtained by three replicate analyses of the concentrations of extracted analytes in real water samples under the optimized condition in one single day and three consecutive days. The intra- and inter-day relative standard deviations (RSDs) were calculated on the basis of the measured peak area ratios. Recoveries of targeted analytes were investigated by extracting the standard spiked water solutions containing 20 μg L^{-1} bifenthrin under the optimized condition, and calculating by comparing the peak areas from the spiked water sample to those obtained from the standard solution at the same concentration.

Application of Nanocomposites to the Analysis of Real Samples

To evaluate the extraction performance of the resultant Fe_3O_4@m-SiO_2/PSA@Zr-MOF nanocomposites in real water samples, pond water and river water were chosen to be the environmental samples in this work. Water samples which contained 20 μg L^{-1} bifenthrin standard solution were investigated. The whole extraction procedure was performed under the optimized conditions.

Results and Discussion

Characterization of Fe_3O_4@m-SiO_2/PSA@Zr-MOF Nanocomposites

The morphologies and the sizes of the resultant Fe_3O_4@m-SiO_2/PSA@Zr-MOF nanocomposites were characterized by SEM and TEM. The SEM image (Fig. 3a) showed that the magnetic nanocomposites were uniform and the average diameter was 510 nm with a narrow size distribution (standard deviation = 7.49%). The TEM image (Fig. 3b) revealed that the resultant nanocomposite was composed of a Fe_3O_4 core and an m-SiO_2/PSA@MOF shell. EDX analysis of the resultant Fe_3O_4@m-SiO_2/PSA@Zr-MOF nanocomposites presented the existence of Si, N and Zr elements, which revealed that m-SiO_2, PSA and Zr-MOF were modified on the Fe_3O_4 cores (Fig. 3c).

The chemical states of elements were further investigated by XPS. Figure 4a displayed the wide-scan XPS

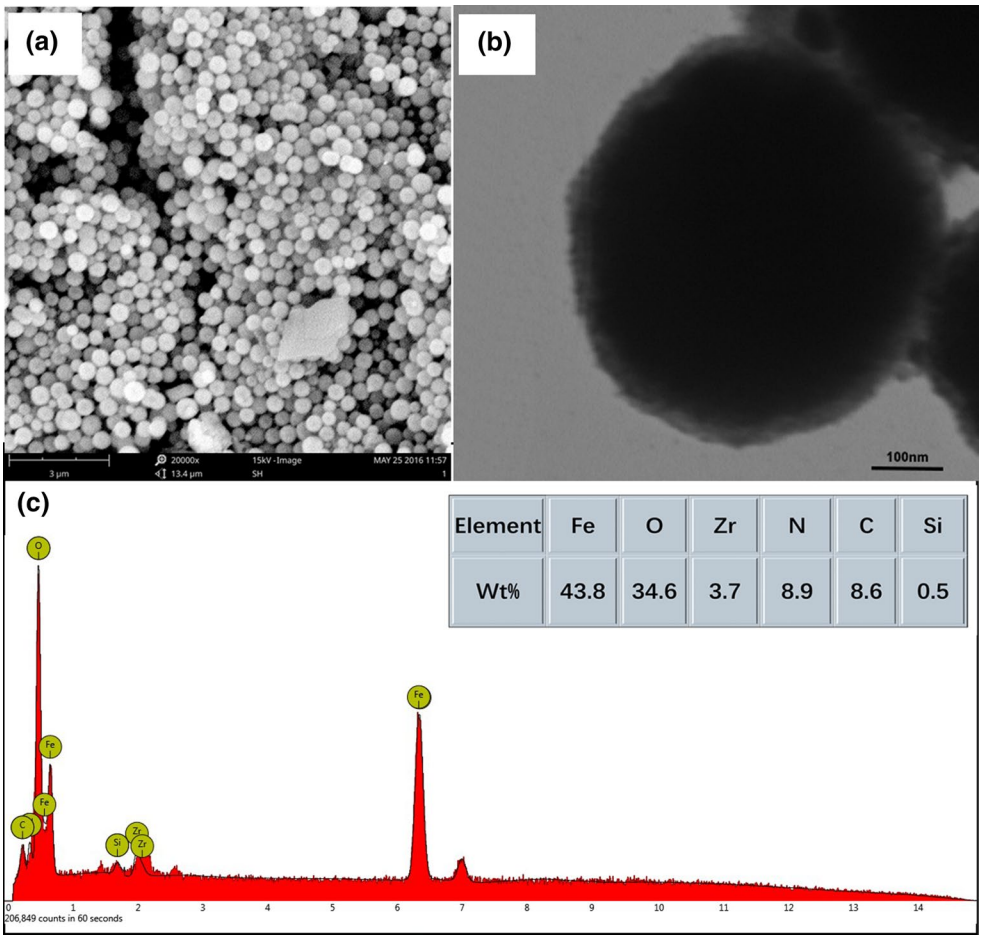

Fig. 3 SEM image (**a** magnification = 20,000, *scale bar* 3 μm), TEM image (**b** magnification = 100,000, *scale bar*100 nm), and EDX spectrum (**c**) of the synthesized Fe_3O_4@m-SiO_2/PSA@Zr-MOF nanocomposites

spectra of the Fe_3O_4@m-SiO_2/PSA and Fe_3O_4@m-SiO_2/PSA@Zr-MOF, which indicated that C1s, O1s and Fe2p were the predominant signals and occurred at 285.65, 533.23 and 713.76 eV, respectively. The peaks at 182.50 and 334.65 eV were assigned to Zr signals, which were derived from Zr-MOF. In the core-level spectrum of Fe2p (Fig. 4b), the peaks of Fe2p3/2 and Fe2p1/2 were located at 711.23 and 724.73 eV, rather than at 710.34 and 724.02 eV (characteristic assignments for γ-Fe_2O_3). The result was well in agreement with the reported data of Fe2p3/2 and Fe2p1/2 for the Fe_3O_4 phase, which revealed the formation of Fe_3O_4 cores in the initial solvothermal reaction [26]. For Fe_3O_4@m-SiO_2/PSA (Fig. 4c), the high-resolution XPS spectrum of the N1s core level was divided into two peaks with binding energy (BE) of 399.71 eV (–NH_2) and 401.68 eV (–NH–), both of which originated from PSA. After further modification with Zr-MOF (Fig. 4d), an additional signal at 402.95 eV (=N–) was shown, which could be attributed to the DMF molecules (which acted as a component in the formation of Zr-MOF). Moreover, the –NH_2 absorption peak moved to a higher BE with a shift of 0.93 eV (from 399.71 to 400.64 eV). The shift phenomenon could be explained as follows: Zr^{4+} had chelated with nitrogen atom (the nitrogen here is derived from the –NH_2 groups and have a couple of isolated electrons), which induced the thickness of the electron clouds around the nitrogen atom to decrease and consequently BE to become higher [27].

The FT-IR spectrum of the resultant Fe_3O_4@m-SiO_2/PSA@Zr-MOF is shown in Fig. 4e. Two strong adsorption bands located at 536 and 3354 cm^{-1} were ascribed to Fe–O–Fe stretching vibration of Fe_3O_4 and O–H stretching vibration of the absorbed water, respectively. The characteristic peak of asymmetric Si–O–Si stretching vibration was observed near 1021 cm^{-1}. The peak that appeared at 1376 cm^{-1} could be attributed to the N–C–H bending mode, which came from PSA and DMF. The vibrations at 1469, 1513 and 1553 cm^{-1} were assigned to the skeletal vibrations of the aromatic ring, which originated from terephthalic acid. In addition, a weak peak around 3029 cm^{-1} could be ascribed to the C–H stretching vibration of the aromatic ring as well.

The typical XRD patterns of Fe_3O_4 (a1), Fe_3O_4@m-SiO_2/PSA (b1) and Fe_3O_4@m-SiO_2/PSA@Zr-MOF (c1) are shown in Fig. 4f. Six Bragg peaks shown their presence at 2θ = 29.99°, 35.24°, 43.00°, 53.66°, 56.92° and 62.65°,

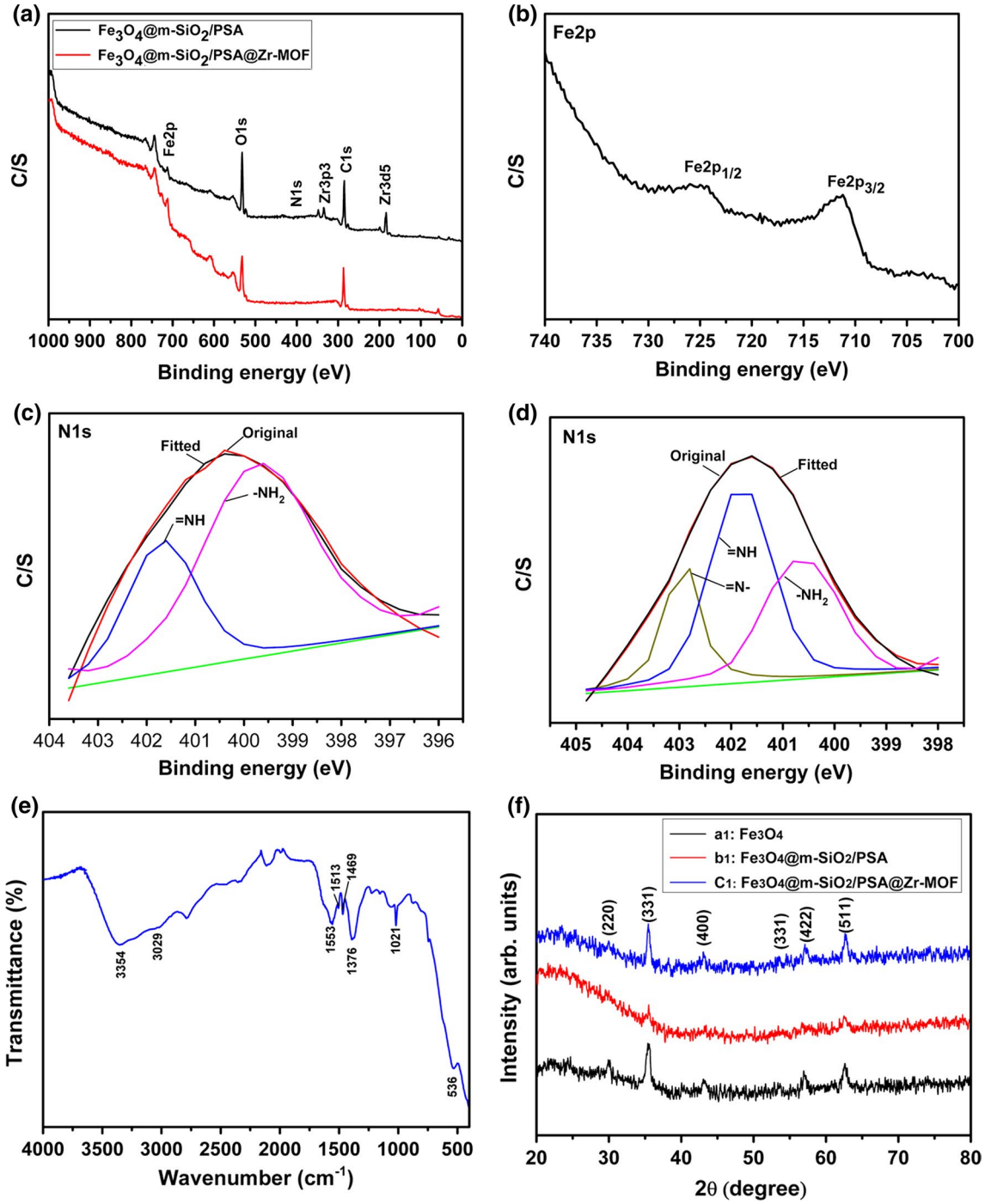

Fig. 4 XPS spectra of **a** wide scan of Fe_3O_4@m-SiO_2/PSA and Fe_3O_4@m-SiO_2/PSA@Zr-MOF; **b** Fe2p core-level spectrum; **c** N1s core-level spectrum of Fe_3O_4@m-SiO_2/PSA; **d** N1s core-level spectrum of Fe_3O_4@m-SiO_2/PSA@Zr-MOF; **e** FT-IR spectrum of Fe_3O_4@m-SiO_2/PSA@Zr-MOF nanocomposites; **f** XRD patterns for (*a1*) Fe_3O_4, (*b1*) Fe_3O_4@m-SiO_2/PSA, and (*c1*) Fe_3O_4@m-SiO_2/PSA@Zr-MOF

which were associated with (220), (331), (400), (311), (422) and (511) planes of the inverse spinel-structured Fe_3O_4. The crystallographic identity of the Fe_3O_4 core was face-centered cubic (FCC) structures based on the standard data of JCPDS file 79-0419, which usually exhibited high magnetic responsivity. Comparing curve (b1–c1) to curve (a1), the spinel structure of Fe_3O_4 was unchanged with the introduction of m-SiO_2, PSA and Zr-MOF (Fig. 5b1–c1).

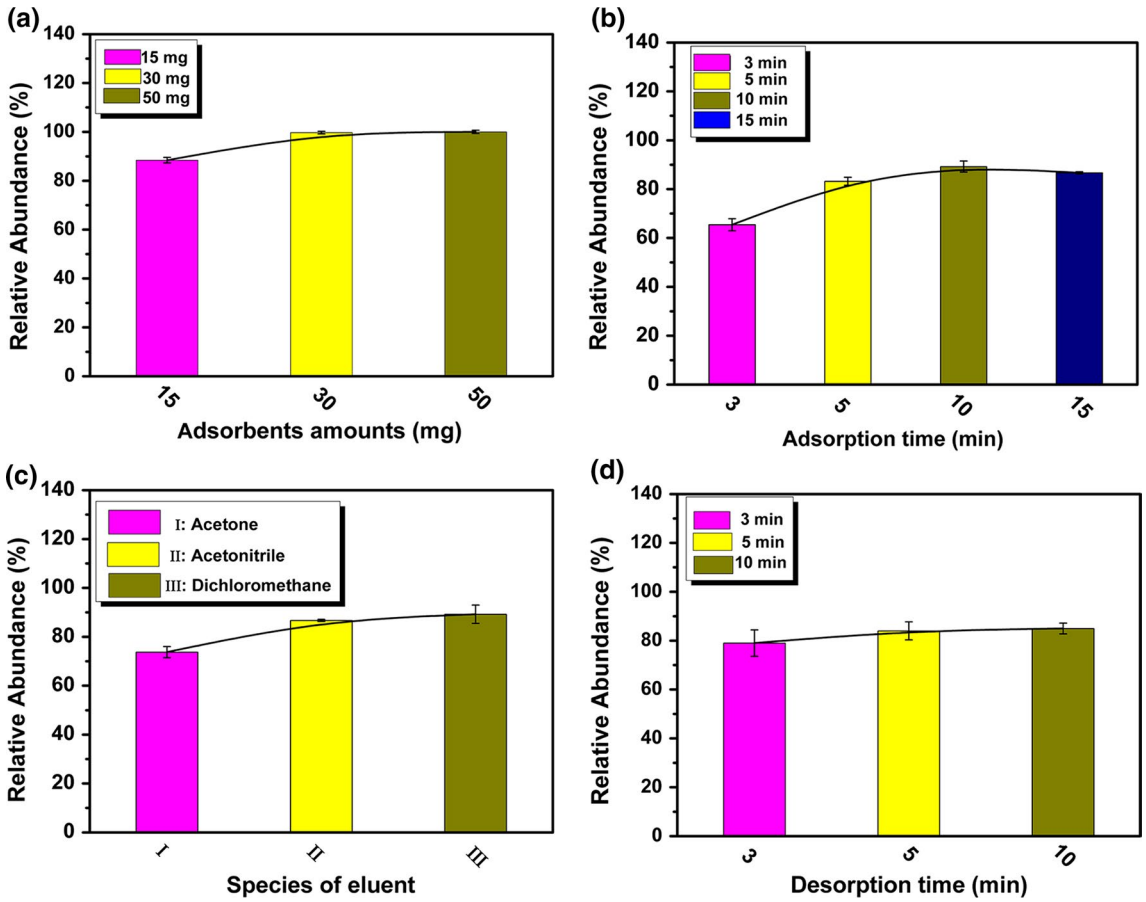

Fig. 5 Optimization of the extraction course: **a** adsorbent amounts (15, 30, 50 mg); **b** adsorption time (3, 5, 10 and 15 min); **c** species of eluents (I: acetone, II: acetonitrile and III: dichloromethane); **d** desorption time (3, 5 and 10 min; $n = 3$)

However, the characteristic peak intensity diffracted from the Fe_3O_4 cores became weak because of the mixed modification of PSA and Zr-MOF.

Optimization of the Extraction Conditions

Benefitting from the unique structures and composition, the Fe_3O_4@m-SiO_2/PSA@Zr-MOF nanocomposites offered the consolidated advantages of Fe_3O_4 MNPs, PSA and Zr-MOF characteristics. The magnetic property of Fe_3O_4 MNPs could simplify the whole extraction procedure by using an external magnetic field; the uniform pore size and large surface area of Zr-MOF provided abundant sites to extract targeted analytes; hydrophilic groups originating from PSA made the resultant adsorbents disperse well in water environments, which could ensure a sufficient contact with the targeted analytes in the aqueous phase. With the aim of improving the extraction performance and simplifying the whole procedures, a series of experimental parameters including adsorbent amounts, adsorption time, species of eluents and desorption time were optimized in our work.

The amount of magnetic adsorbents is mainly determined by the bifenthrin quantity and can largely influence the extraction efficiency. In this work, the adsorbent amounts were studied at three levels (15, 30 and 50 mg). As shown in Fig. 5a, when the amount of Fe_3O_4@m-SiO_2/PSA@Zr-MOF nanocomposites reached 30 mg, it was enough for bifenthrin extraction and there was no significant difference between 30 and 50 mg. Therefore, 30 mg was considered to be the optimized adsorbent amount. Simultaneously, the adsorption time is another important parameter in the adsorption course, which can guarantee a sufficient contact between adsorbents and targeted analytes. The effect of adsorption time in the range of 3–15 min is shown in Fig. 5b. With an extending time from 3 to 10 min, the recoveries of bifenthrin increased. As time was further prolonged to 15 min, there was no obvious improvement due to the rapid distribution of the adsorbents in the aqueous phase. As a result, 10 min was designed as the best adsorption time.

The desorption course also plays an important role in the whole extraction procedure. During the desorption course, there are two parameters required to be optimized. Here, three types of solvents, namely, acetone, acetonitrile and dichloromethane, were experimented to investigate the desorption effect, and the results are shown in Fig. 5c. It was found that acetonitrile and dichloromethane had similar eluting performance, both of which exhibited higher eluting effect than acetone. Between acetonitrile and dichloromethane, we selected acetonitrile as the eluent in the following work, because it had a relatively stable recovery (error bar was smaller). The high eluting efficiency of acetonitrile could be ascribed to its similar polarity to the targeted analytes. The desorption time was another important factor needed to be optimized. A variety of desorption times ranging from 3 to 10 min were studied. Figure 5d revealed that 5 min was enough to elute the bifenthrin absorbed by adsorbents. On prolonging to 10 min, no obvious increase occurred. Moreover, continuous ultrasonication for a long time may cause shell-layer delamination or structural change of the magnetic adsorbents. Hence, 5 min was identified as the optimized desorption time. During the whole extraction procedures, 30 mg absorbents, 10 min adsorption time, acetonitrile as eluent and 5 min desorption time were selected as the optimized conditions for further work.

Method Validations

Method validations including linear range, correlation coefficient (R^2), LOD, LOQ and reproducibility were studied under the optimized conditions. As summarized in Table 1, good linearity was obtained and the corresponding R^2 was 0.9998. The LOD value was 0.5 μg L^{-1} on the basis of $S/N = 3$, and the LOQ based on $S/N = 10$ was 1.5 μg L^{-1}. Precision of the proposed method was evaluated by the intra- and inter-day RSD, and the values were 2.0 and 3.5%, respectively, revealing an acceptable reproducibility. In addition, the recovery of bifenthrin was 103.2%. All the results demonstrated that the proposed method based on the MSPE technique was efficient and reliable.

Table 1 The validation data of MSPE–GC–MS procedure

Items	Values
Calibration curves	$y = 0.03886x + 0.02976$
R^2	0.9998
Linear range	3.3–200 μg L^{-1}
LOD; LOQ ($n = 3$)	0.5; 1.5 μg L^{-1}
Intra-day RSD; inter-day RSD ($n = 3$)	2.0%; 3.5%
Recovery ($n = 3$)	103.2%

Application in Real Water Samples

Inspired by the satisfying results above, Fe_3O_4@m-SiO_2/PSA@Zr-MOF nanocomposites were applied to the extraction of bifenthrin in pond water as well as river water samples. No bifenthrin was detected in pond water, while it was found in river water. Figure 6a, b compares the GC–MS chromatogram of the river water sample with that of bifenthrin-spiked river water. The results indicated that bifenthrin at a low concentration of 1.4 ± 0.1 μg L^{-1} was detected in the river water, despite its complex matrix. The comparison indicated that the resultant Fe_3O_4@m-SiO_2/PSA@Zr-MOF nanocomposites exhibited excellent extraction ability toward bifenthrin in real water samples. Moreover, the synthesized adsorbents had a satisfactory magnetic responsivity; they could be rapidly separated in only 15 s by an external magnetic field.

A comparison of the proposed method with published analytical works for the determination of bifenthrin is represented in Table 2. The method in our work had comparable or even lower RSD than these reported methods.

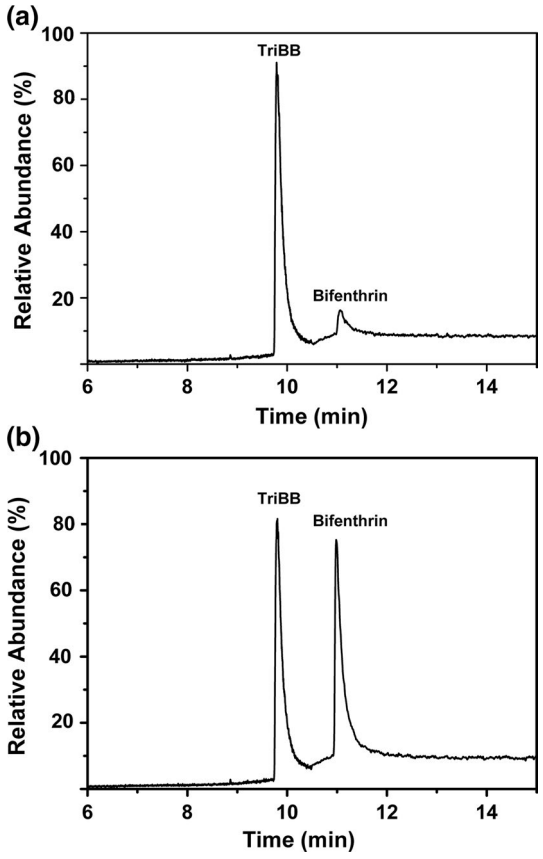

Fig. 6 The representative GC–MS chromatograms of **a** river water sample and **b** 20 μg L^{-1} bifenthrin-spiked river water sample by the developed method

Table 2 Comparison of different methods for bifenthrin extraction in water environments

Extraction methods	RSD (%)	Recovery (%)	Sample volume (mL)	Extraction time (min)	Solvent volume (mL)	References
MSPE–GC–MS	2.0	103	15	10	1.0	This work
MSPE–UFLC-UV	3.3	80.6	100	20	3.0	[28]
LLE–GC–ECD	0.98	104.6	>500	>20	>60	[29]
SPE–LC/ESI–MS	3.8	105.4	800	>130	>200	[30]

Meanwhile, the proposed method was facile and time saving, and only consumed 10 min of the whole extraction process. Less than 1.0 mL organic solvent was needed, indicating that this method was safe and environment-friendly. Moreover, the whole extraction process was conducted without any special equipment. All the results revealed that the proposed method based on Fe_3O_4@m-SiO_2/PSA@Zr-MOF absorbents was feasible and reliable for the determination of bifenthrin in water samples.

Conclusions

In this study, magnetic adsorbents based on Fe_3O_4 MNPs were successfully synthesized. Due to the special structure and composition, the Fe_3O_4@m-SiO_2/PSA@Zr-MOF nanocomposites could easily monodisperse in the aqueous phase and be separated rapidly with the aid of the external magnetic bar. The resultant nanocomposites showed great potential as MSPE adsorbents. A variety of extraction parameters influencing the extraction efficiency were studied, including the amounts of magnetic adsorbents, the adsorption time, the types of eluents and the desorption time. The optimized conditions were as follows: absorbent amounts, 30 mg; adsorption time, 10 min; species of eluents, acetonitrile; desorption time, 5 min. Eventually, the developed method was successfully applied to the extraction and analysis of bifenthrin in real water samples. The results indicated that the novel approach offered an attractive alternative for rapid, convenient, efficient and selective method for the determination of bifenthrin in water samples, and it can be predicted that the proposed method may be extended to other types of targeted analytes and matrix samples.

Acknowledgements This study was supported in parts by the Key Laboratory of Cigarette Smoke, Technology Center of Shanghai Tobacco (Group) Corp, and the Natural Science Foundation of China (Grant No. 41322024). The authors also thank Enriching Biotechnology (Shanghai) for materials support.

Compliance with Ethical Standards

Conflict of interest The authors declare that there are no conflicts of interest.

References

1. Djordjevic T, Djurovic R, Gajic Umiljendic J (2012) Pestic Phytomed (Belgrad) 27:167–174
2. Luo YB, Li X, Jiang XY, Cai BD, Zhu FP, Zhang HF, Chen ZG, Pang YQ, Feng YQ (2015) J Chromatogr A 1406:1–9
3. Savia GD, Piacentinia KC, Bortolottob T, Scussela VM (2016) Food Chem 203:246–251
4. VanDusen AE, Richards SL, Balanay JAG (2015) Pest Manag Sci. doi:10.1002/ps.4081
5. Mostafalou S, Abdollahi M (2013) Toxicol Appl Pharm 268:157–177
6. Beketov MA, Kefford BJ, Schafer RB, Liess M (2013) Proc Natl Acad Sci 110:11039–11043
7. Tewary DK, Kumar V, Ravindranath SD, Shanker A (2005) Food Control 16:231–237
8. Ranjbari E, Hadjmohammadi MR (2012) Talanta 100:447–453
9. Jara S, Lysebo C, Greibrokk T, Lundanes E (2000) Anal Chim Acta 407:165–171
10. Jimenez FJL, Rubio S, Bendito DP (2005) Anal Chim Acta 551:142–149
11. Ma YR, Zhang XL, Zeng T, Cao D, Zhou Z, Li WH, Niu HY, Cai YQ (2013) ACS Appl Mater Interfaces 5:1024–1030
12. Lin JH, Wu ZH, Tseng WL (2010) Anal Methods 2:1874–1879
13. Zhang XL, Niu HY, Pan YY, Shi YL, Cai YQ (2011) J Colloid Interface Sci 362:107–112
14. Xu LN, Qi XY, Li XJ, Bai Y, Liu HW (2016) Talanta 146:714–726
15. Hana Q, Wang ZH, Xia JF, Chen S, Zhang XQ, Ding MY (2012) Talanta 101:388–395
16. Wang P, Lo IMC (2009) Water Res 43:3727–3734
17. Ye Q, Chen ZB, Liu LH, Hong LM (2016) Anal Methods 8:3391–3396
18. Xu M, Liu MH, Sun MR, Chen K, Cao XJ, Hu YM (2016) Talanta 150:125–134
19. Wang XY, Deng CH (2016) Talanta 148:387–392
20. Wang WN, Ma RY, Wu QH, Wang C, Wang Z (2013) Talanta 109:133–140
21. Sun YY, Tian J, Wang L, Yan HY, Qiao FX, Qiao XQ (2015) J Chromatogr A 1422:53–59
22. Wang XY, Deng CH (2015) Talanta 144:1329–1335
23. Stock N, Biswas S (2011) Chem Rev 112:933–969
24. Huo SH, Yan XP (2012) Analyst 137:3445–3451
25. Zhao H, Hou L, Wu JX, Lu YX (2016) J Mater Chem. doi:10.1039/c6tc01979j
26. Li J, Zhang S, Chen C, Zhao G, Yang X, Li J, Wang X (2012) ACS Appl Mater Interfaces 4:4991–5000
27. Zhao H, Lu YX (2016) Appl Surf Sci 362:154–162
28. Yu X, Sun Y, Jiang CZ, Sun XM, Gao Y, Wang YP, Zhang HQ, Song DQ (2012) Talanta 98:257–264
29. Wu J, Lu J, Wilson C, Lin YJ, Lu H (2010) J Chromatogr A 1217:6327–6333
30. Garcia MDG, Martinez DB, Galera MM, Vazquez PP (2006) Rapid Commun Mass Spectrom 20:2395–2403